# Multi-Stage Data Fusion in Security and Defence

**Stefano Coraluppi**
NATO Undersea Research Centre
Viale S. Bartolomeo 400, 19126 La Spezia
ITALY

E-mail: coraluppi@nurc.nato.int

## *ABSTRACT*

*The fundamental problem of target tracking is to estimate the state of one or more objects that persist over time, based on noisy measurements contained in a vast quantity of mostly spurious measurement data. Target tracking is closely related to a number of basic problems in statistical modelling and information extraction from noisy data. Multi-stage processing provides a wealth of processing options that can be exploited to achieve robust and high-performance surveillance. This manuscript describes a number of multi-stage tracking architectures that the author has recently studied. Additionally, we study the target cardinality problem.*

## 1 INTRODUCTION

Tracking combines estimation theory and detection theory, with the further complication of measurement origin uncertainty. Table 1 identifies a number of fundamental problems in information extraction from noisy data.

**Table 1.1: A taxonomy of information extraction problems in target tracking. The problems noted in boldface are addressed in this lecture.**

| Number of targets | Number of targets | False contacts | Target motion | Solution methodology |
|---|---|---|---|---|
| single | known | no | parametric | non-Bayesian estimation (least squares) |
| single | known | no | stochastic | Bayesian estimation (nonlinear filtering) |
| single | known | yes | parametric | non-Bayesian estimation (maximum-likelihood tracking) |
| single | known | yes | stochastic | Bayesian estimation (single-target track maintenance) |
| multiple | known | yes | stochastic | Bayesian estimation (multi-target track maintenance) |
| multiple | unknown | yes | N/A | Bayesian estimation (**target cardinality**) |
| multiple | unknown | yes | stochastic | Hypothesis testing & Bayesian estimation (**coupled track management & track maintenance**) |

As we see from table 1.1, many of the solution methodologies relevant to the surveillance problems of interest rely on estimation and detection theory. Here, we will focus on our recent work in the last two

problem domains listed in table 1.1. First, in section 2, we study the target cardinality problem. Next, in section 3, we overview a number of multi-stage and multi-hypothesis data fusion architectures that we have developed in recent years, and provide details and examples for some of these.

# 2 THE TARGET CARDINALITY PROBLEM

Many of the problems in table 1.1 involve the application of estimation theory for determining *where* a target or multiple targets are to be found, assuming that the number of targets is *known*. Now we wish to determine the number of targets, i.e. target *cardinality*, disregarding the question of *where* targets are located. The solution to this problem constitutes a further application of estimation theory.

## 2.1 The static problem

Assume that the surveillance region contains $N_T$ target, where $N_T \sim Poisson(\lambda_T)$. That is,

$$p(N_T = n_T) = \frac{\lambda_T^{n_T}}{n_T!}\exp(-\lambda_T),\ n_T \geq 0. \tag{2.1}$$

Further, assume that targets are detected with probability *p*. Invoking the splitting property of the Poisson process [1], we have that the probability distribution for the number of target contacts $N_C$ is given by $N_C \sim Poisson(p\lambda_T)$:

$$p(N_C = n_C) = \frac{(p\lambda_T)^{n_T}}{n_T!}\exp(-p\lambda_T),\ n_C \geq 0. \tag{2.2}$$

A question of interest is the following: what is the probability distribution on $N_T$, given that $n_C$ contacts are observed? The distribution of interest can be obtained by use of Bayes' rule and the probability distribution of $N_C$ given $N_T$, which is given by the binomial distribution.

$$p(N_T = n_T \mid N_C = n_C) = \frac{p(N_C = n_C \mid N_T = n_T)p(N_T = n_T)}{p(N_C = n_C)},\ n_T \geq n_C. \tag{2.3}$$

$$p(N_C = n_C \mid N_T = n_T) = \binom{n_T}{n_C} p^{n_C}(1-p)^{n_T - n_C},\ n_C \geq 0 \text{ and } n_C \leq n_T. \tag{2.4}$$

Manipulation of (2.1-2.4) yields the following.

$$p(N_T = n_T \mid N_C = n_C) = \frac{((1-p)\lambda_T)^{n_T - n_C}\exp(-(1-p)\lambda_T)}{(n_T - n_C)!},\ n_T \geq n_C. \tag{2.5}$$

That is, having observed $n_C$ contacts, the number of targets equals or exceeds $n_C$ with a probability that is prescribed by (2.5); thus $N_T = n_C + r$, where $r \sim Poisson((1-p)\lambda_T)$. This is a nice result, in that the number of unobserved targets obeys the same probability distribution as we had *a priori*, albeit with a suitably reduced mean.

**Remark 2.1** For some surveillance problems, notably in the mine-warfare community, the *Poisson prior* assumption is not always invoked. The assumption of a *uniform prior* leads to a *negative binomial* distribution [2]. Modifications to the uniform prior have been considered to reason over multiple surveillance regions [3]. Another philosophy for choosing the prior distribution leads to the *Katz distribution* [4].

**Remark 2.2** One criticism of the Poisson distribution is that does not address the interdependencies that may exist with respect to target presence. In some applications, as in mine warfare, it is found empirically that the conditional distribution on undetected targets depends on the number of detected targets: targets exist in clusters. A second criticism is that, as a one-parameter distribution, its variance cannot be set independently of the mean (they are the same), and thus does not accurately reflect uncertainty.

**Remark 2.3** An important characteristic of the solution given by (2.5) is that it is consistent with respect to partitioning of the surveillance region. That is, consider two non-overlapping regions with priors $\lambda_{T1}$ and $\lambda_{T2}$, in which we observe $n_{C1}$ and $n_{C1}$ targets, respectively. Assuming the same detection probability $p$ applies to both regions, we have $N_{T1} = n_{C1} + r_1$ and $N_{T2} = n_{C2} + r_2$, where $r_1 \sim Poisson((1-p)\lambda_{T1})$ and $r_2 \sim Poisson((1-p)\lambda_{T2})$. Summing these results, we have $N_{T1} + N_{T2} = n_{C1} + n_{c_2} + r$, where $r = r_1 + r_2 \sim Poisson((1-p)(\lambda_{T1} + \lambda_{T1}))$ using the merging property of the Poisson process [1]. This is the same result that one obtains by considering a single surveillance region given by the union of the two surveillance regions.

We now consider the multi-sensor (or multi-scan) problem, in which a region with a fixed number of targets $N_T$ is observed $S$ times, resulting in a *sequence* of detection cardinalities that we denote by $n_C = (n_{C1}, n_{C2}, ..., n_{CS})$. We are interested in the same question as before: what is the probability distribution on $N_T$, given that the sequence $n_C$ is observed?

The measurements in the sequence $n_C$ are conditionally independent, given the number of targets $N_T$. Accordingly, (2.4) can easily be replaced by (2.7). Then, applying Bayes' rule, the probability distribution on $N_T$ given that the sequence $n_C$ is observed is given by (2.8), which relies on (2.1) and (2.7).

$$p(N_C = n_C \mid N_T = n_T) = \prod_{i=1}^{S} \binom{n_T}{n_{Ci}} p^{n_{Ci}} (1-p)^{n_T - n_{Ci}}, \; n_{Ci} \geq 0 \forall i \text{ and } \max_i \{n_{Ci}\} \leq n_T. \tag{2.7}$$

$$p(N_T = n_T \mid N_C = n_C) = \frac{p(N_C = n_C \mid N_T = n_T) p(N_T = n_T)}{\sum_{j=\max_i \{n_{Ci}\}}^{\infty} p(N_C = n_C \mid N_T = j) p(N_T = j)}, \; n_T \geq \max_i \{n_{Ci}\}. \tag{2.8}$$

Unfortunately, the posterior probability distribution given by expression (5.8) does not lend itself to a simple interpretation as we had with (2.5).

**Remark 2.4** A recursive implementation of (2.8) is possible. Let $n_C^- = (n_{C1}, n_{C2}, ..., n_{C(S-1)})$, so that $n_C = (n_C^-, n_{CS})$. Then, using the conditional independence of measurements in the sequence $n_C$ given the number of targets, (2.9) results.

$$\begin{aligned} p(N_T = n_T \mid N_C = n_C) &= \frac{p(N_{CS} = n_{CS} \mid N_C^- = n_C^-, N_T = n_T) p(N_T = n_T \mid N_C^- = n_C^-)}{\sum_{j=\max\left\{n_{Cs}, \max_{i\in\{1,...,S-1\}} n_{ci}\right\}}^{\infty} p(N_{CS} = n_{CS} \mid N_C^- = n_C^-, N_T = j) p(N_T = j \mid N_C^- = n_C^-)} \\ &= \frac{p(N_{CS} = n_{CS} \mid N_T = n_T) p(N_T = n_T \mid N_C^- = n_C^-)}{\sum_{j=\max\left\{n_{Cs}, \max_{i\in\{1,...,S-1\}} n_{ci}\right\}}^{\infty} p(N_{CS} = n_{CS} \mid N_T = j) p(N_T = j \mid N_C^- = n_C^-)}. \end{aligned} \tag{2.9}$$

Having determined the posterior probability distribution as prescribed by (2.5), (2.8), or (2.9), we are now in the position to estimate the target cardinality. We can do so with a number of Bayesian estimators, including MMSE, MMAE, and MAP. The MAP estimator is the simplest, as maximization of the posterior distribution over $n_T$ does not require computation of the denominator in (2.5), (2.8), or (2.9).

## 5.2 The static problem with false alarms

We consider now a generalization of the problem considered in section 5.1. Again, we have an unknown number of targets with prior distribution given by $N_T \sim Poisson(\lambda_T)$. At each scan, in addition to target detections which occur with probability $p$ for each target, we observe a number of false returns with prior distribution $N_{FA} \sim Poisson(\lambda_{FA})$. As before, we observe a sequence of $S$ detection cardinalities given by

$n_C = (n_{C1}, n_{C2}, ..., n_{CS})$. What is the probability distribution on $N_T$, given that the sequence $n_C$ is observed?

It turns out that this problem can be answered with minor modifications to our previous results, by conditioning on the number of returns that are target-induced in each scan to obtain (2.10).

$$p(N_C = n_C \mid N_T = n_T) = \prod_{i=1}^{S} \sum_{j=1}^{n_T} \left( \frac{\lambda_{FA}^{n_C - j} \exp(-\lambda_{FA})}{(n_{Ci} - j)!} \cdot \binom{n_T}{j} p^j (1-p)^{n_T - j} \right), \; n_{Ci} \geq 0 \forall i, \; n_T \geq 0. \tag{2.10}$$

$$p(N_T = n_T \mid N_C = n_C) = \frac{p(N_C = n_C \mid N_T = n_T) p(N_T = n_T)}{\sum_{j=0}^{\infty} p(N_C = n_C \mid N_T = j) p(N_T = j)}, \; n_T \geq 0. \tag{2.11}$$

In the single-scan case, applying both the merging and splitting properties of the Poisson process, the denominator in (2.11) can be expressed more simply according to (2.12).

$$p(N_C = n_C) = \frac{(\lambda_{FA} + p\lambda_T)^{n_C}}{n_C!} \exp(-\lambda_{FA} - p\lambda_T), \; n_C \geq 0. \tag{2.12}$$

As before, once the posterior probability distribution is defined, Bayesian estimators can be readily computed.

**Remark 2.5** In the mine-warfare community, the general problem with false alarms is not usually considered [2-4]. The reason for this is that detection processing includes close inspection of suspected mines, so that false alarm rates are negligible. Nonetheless, the generalization is of interest in other surveillance settings.

**Remark 2.6** As before, a recursive computation of the posterior probability distribution for $N_T$ is possible, according to (2.13).

$$p(N_T = n_T \mid N_C = n_C) = \frac{p(N_{CS} = n_{CS} \mid N_T = n_T) p(N_T = n_T \mid N_C^- = n_C^-)}{\sum_{j=0}^{\infty} p(N_{CS} = n_{CS} \mid N_T = j) p(N_T = j \mid N_C^- = n_C^-)}. \tag{2.13}$$

### 5.3 The dynamic problem

We consider now a generalization of the target cardinality problem, whereby the number of targets is time-varying, as specified by birth and death processes. In particular, assume that, at each scan, the number of target births is Poisson distributed with parameter $\lambda_B$, and that the number of target deaths is Poisson distributed with parameter $q \cdot \lambda_T$, i.e. at each scan each existing targets dies with probability $0 \leq q \leq 1$. Once more, we observe a sequence of *S* detection cardinalities given by $n_C = (n_{C1}, n_{C2}, ..., n_{CS})$, and we wish to determine the probability distribution on $N_T$, given that the sequence $n_C$ is observed.

In the absence of cardinality measurements, the steady-state target distribution is uniquely determined by the parameters $\lambda_B$ and $q$. In particular, equating the birth and death rates, equation (2.14) follows. Thus, we assume that the prior target cardinality is given by $N_T \sim Poisson(\lambda_T)$, with $\lambda_T$ consistent with (2.14).

$$\lambda_T = \frac{\lambda_B}{q}. \tag{2.14}$$

**Remark 2.7** More generally, given a target distribution with parameter $\lambda_0$, after *k* scans we have (2.15). It is easy to show from (2.15) that, for $k \to \infty$, we have $\lambda(k) \to \lambda_T$. It is interesting to note that arbitrarily long *back-prediction* consistent with the dynamics (2.15) is only possible for target densities that exceed $\lambda_T$. The back-prediction equation and the associated back-prediction limit are given by (2.16-2.17). Note that the limit in (2.17) only applies to target cardinalities lower that the steady-state solution; when these are larger, arbitrarily large back-predictions are possible.

$$\lambda(k) = \lambda_0 (1-q)^k + \sum_{i=0}^{k-1} \lambda_B (1-q)^i \,. \tag{2.15}$$

$$\lambda_0 = \frac{\lambda(k) - \sum_{i=0}^{k-1} \lambda_B (1-q)^i}{(1-q)^k} \,. \tag{2.16}$$

$$\lambda_0 > 0 \Leftrightarrow \lambda(k) > \sum_{i=0}^{k-1} \lambda_B (1-q)^i \Leftrightarrow \lambda(k) > \lambda_B \frac{1-(1-q)^k}{q} \Leftrightarrow k < \frac{\log\left(1 - \frac{q\lambda(k)}{\lambda_B}\right)}{\log(1-q)} \text{ for } \lambda(k) < \frac{\lambda_B}{q} \,. \tag{2.17}$$

We now develop a recursive expression for the posterior distribution on target cardinality, given by (2.18-2.19). Compared with (2.9), it requires the diffusion or prediction equation (2.18), which involves conditioning on the number of targets that survive from the previous scan. Equation (2.19) involves conditioning on the previous target cardinality; note that, due to the death process, only the last measurement is relevant for providing a lower bound on target cardinality. Equation (2.19) requires (2.4).

$$p\left(N_{TS} = j \mid N_{T(S-1)} = i\right) = \sum_{k=0}^{i} q^{i-k} (1-q)^k \frac{\lambda_B^{j-k} \exp(-\lambda_B)}{(j-k)!} \tag{2.18}$$

$$p\left(N_{TS} = n_{TS} \mid N_C = n_C\right) = \frac{p\left(N_{CS} = n_{CS} \mid N_{TS} = n_{TS}\right) \sum_{i=0}^{\infty} p\left(N_{TS} = n_{TS} \mid N_{T(S-1)} = i\right) p\left(N_{T(S-1)} = i \mid N_C^- = n_C^-\right)}{\sum_{j=n_{CS}}^{\infty} p\left(N_{CS} = n_{CS} \mid N_{TS} = j\right) \sum_{i=0}^{\infty} p\left(N_{TS} = j \mid N_{T(S-1)} = i\right) p\left(N_{T(S-1)} = i \mid N_C^- = n_C^-\right)} \,. \tag{2.19}$$

Finally, we consider a further generalization to include both cardinality dynamics and false alarms. Equations (2.18-2.19) are directly applicable; in (2.19), in place of (2.4), we use (2.20) – the single-scan version of equation (2.10).

$$p\left(N_C = n_C \mid N_T = n_T\right) = \sum_{j=1}^{n_T} \left( \frac{\lambda_{FA}^{n_C - j} \exp(-\lambda_{FA})}{(n_{Ci} - j)!} \cdot \binom{n_T}{j} p^j (1-p)^{n_T - j} \right), \; n_C \geq 0 \,, \; n_T \geq 0 \,. \tag{2.20}$$

# 3 RECENT ADVANCES IN MULTI-STAGE TRACKING

Among the known approaches to multi-target tracking, multi-hypothesis tracking (MHT) appears to provide the best performance results, albeit at the cost of increased computational expense and with some (generally minor) time latency between the input and output. However, single-stage centralized MHT processing does not suffice in a number of surveillance settings. Table 3.1 lists a number of multi-stage fusion architectures that we have studied, with a brief mention of their applicability. Further details on our MHT algorithm and on many of the multi-stage architectures listed in table 3.1 may be found in [5] and references therein, as well as in more recent papers [6-7].

**Table 3.1: Multi-stage data fusion architectures.**

| Architecture | Applicability |
|---|---|
| track-while-fuse | Baseline, centralized MHT approach [5] |
| track-before-fuse | High detection-threshold settings with pronounced target-fading effects, as in undersea surveillance [5] |
| fuse-before-track | Large sensor networks with synchronized sensors; simplest first-stage static-fusion approach is contact sifting [5] |
| track-extract-track | Dim targets in clutter [5] |
| track-break-fuse | Dense target scenarios [5] |
| modified fuse-before-track | Large sensor networks with synchronized sensors; approaches include ML-MHT, ML-MHT$^2$, and MHT$^2$ [6] |
| track-segment-fuse | Dense target scenarios with lengthy group motion and low-revisit rate feature-rich sensors (see below; closely related to the approach described in [8]) |
| modified track-before-fuse | Multi-sensor settings where feature-rich sensors have low revisit rates or intermittent coverage, requiring customized track-management logic [7] |
| track-adapt-track | Low-resolution sensor settings (see below) |
| low-q track – high-q track | Dim targets in clutter (see below) |
| track merging | Post-processing clean-up procedure that relaxes single-detection assumption (see below) |

The motivation at the heart of all the multi-stage approaches outlined in table 3.1 is to identify multi-stage approaches that match or exceed the performance and robustness characteristics of much more complex single-stage tracking solutions. Further, the MHT algorithmic module at the heart of these architectures is highly modular, thus providing simplicity and flexibility of use in addressing problems in a wide range of surveillance settings. We discuss some recent developments below.

## 3.1 Hypothesis management in dense-target scenarios (*track-segment-fuse*)

As a computationally-efficient variation on the track-break-track architecture [5], we may consider the following scheme. A first MHT stage (with n-scan=0) identifies high-quality contact data. Subsequently, data associations are broken *only* when group compositions change. That is, in the second pass, all tracks are grouped by normalized state proximity and, when a new track enters or leaves a particular group, all tracks in the group are terminated and re-initialized. The resulting set of segmented tracks is then passed to a third processing stage: an MHT stage (with n-scan>>0) that performs segment-to-segment fusion with the inclusion of low-revisit rate feature-rich data. This processing scheme is closely related to that developed in [7], but without the need for aggregate group state computations.

The *track-segment-fuse* approach is preferable to the *track-break-fuse* approach when a high down-stream *n-scan* is required or when multi-target association ambiguities persist for many sensor scans. The *modified fuse-before-track* approaches (see table 3.1) are of intermediate complexity between the others, as track breaks are introduced for at each time step: fewer breaks than in *track-break-fuse*, but more than in *track-segment-fuse*.

## 3.2 Tracking with low-resolution sensors (*track-adapt-track*)

During recent NURC at-sea experimentation, the modified track-before-fuse architecture was severely tested due to the limited resolution of legacy ship-based radar systems [8]. In particular, we find that vessel radar tracks are recently dropped when in close proximity to another. Subsequent to the at-sea experimentation, we have examined this problem further in a simulation-based setting. In particular, we simulate a rendezvous-at-sea whereby targets approach, move in close proximity for some time, and then diverge. Contact data is simulated with a nominal FAR but with a PD that drops significantly while the targets are close.

One approach to this problem is to consider an adaptive track coasting scheme whereby tracks in close proximity are coasted for much longer times in the absence of a measurement update. This approach is problematic, as tracks are easily seduced by false contacts. A more robust approach is to allow track terminations after short-duration coasts, followed by adaptive coasting in a second stage. An illustration of the effectiveness of the two-stage, *track-adapt-track* approach is shown in figures 3.1-3.2.

There is still a need for further improvement to the track-adaptive-track scheme. Indeed, note in the example that, while we are able successfully to associate two track segments on either side of the close-target motion, the other two segments are not successfully associated. Indeed, it is necessary to augment the second-stage adaptive coasting so that the current coasting methodology based on a nearly-constant velocity target motion model (which amounts to dead-reckoning) be replaced by a more sophisticated approach that coasts the track in vicinity of existing active tracks, where these exist. This would allow for maneuvers as part of the track-coasting process.

## 3.3 Tracking dim targets in clutter (*low-q track – high-q track*)

Tracking low PD targets in clutter is a significant challenge. Maximum likelihood (ML) approaches effectively lower the target process noise to zero, and limit the search to a single non-manuevering target. Recently, there has been work to extend ML-based approaches to handle multiple, maneuvering target.

The MHT solution provides a useful tool to address the dim-target challenge. In particular, we proceed in a two-stage approach. In the first stage, we process the data with near-zero process noise. In the second stage, we allow for much lengthier track coasts (as previously done, this is best performed in a downstream stage with less clutter), as well as with a larger process noise. The idea is to associate short, low-maneuver segments into higher-continuity tracks. An illustration of the potential of this approach is given in figures 3.3-3.6.

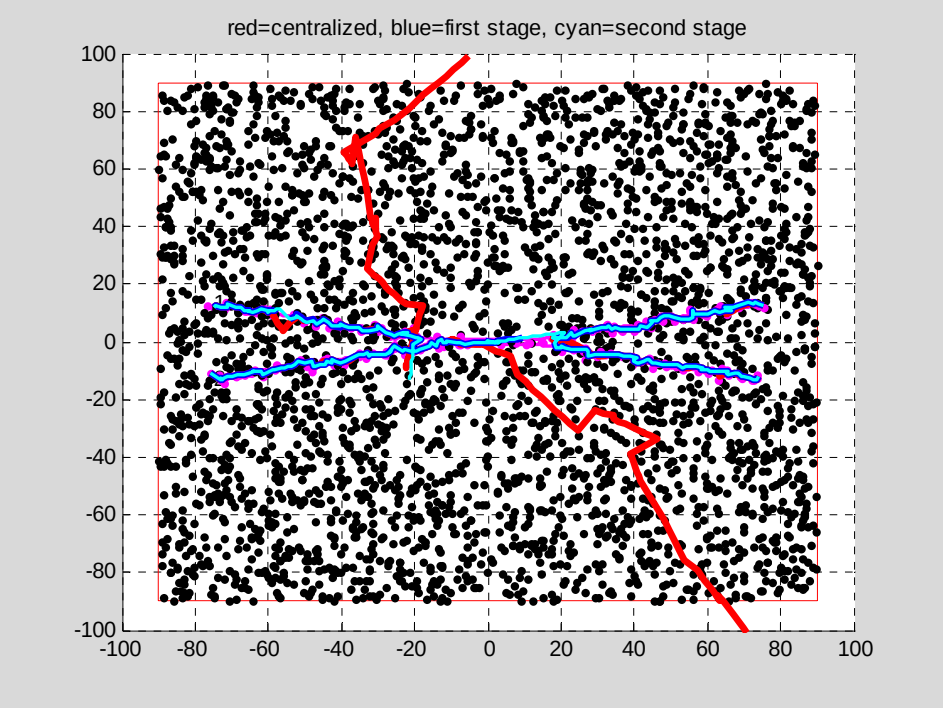


**Figure 3.1: Crossing target trajectories (magenta), contact data (black), single-stage adaptive tracking (red), first-stage tracking (blue), *track-adapt-track* (cyan).**

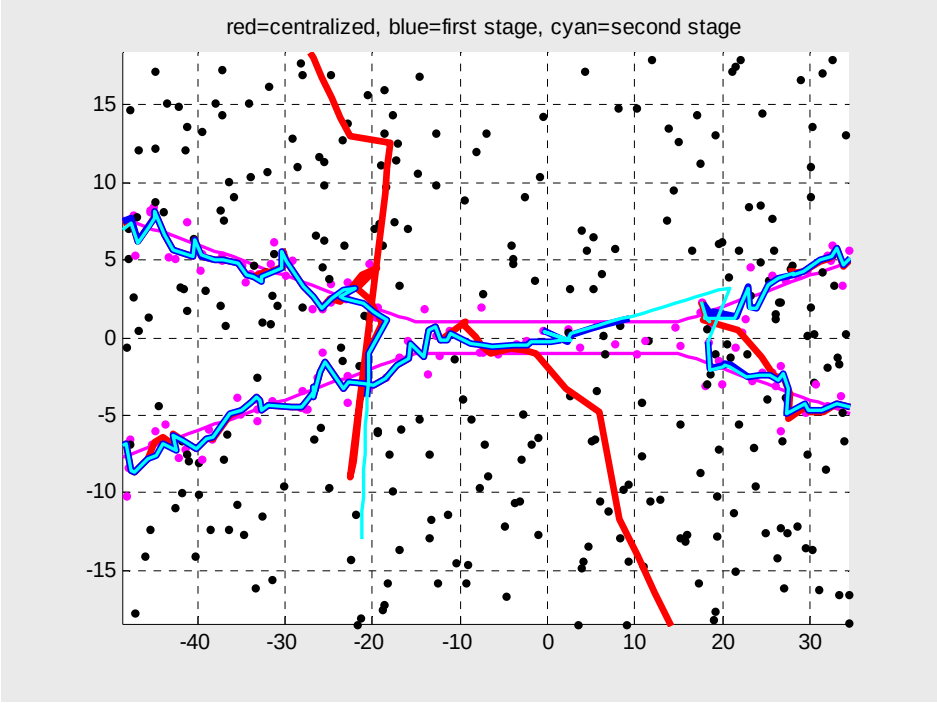


**Figure 3.2: Close-up of crossing target trajectories (magenta), contact data (black), single-stage adaptive tracking (red), first-stage tracking (blue), *track-adapt-track* (cyan).**

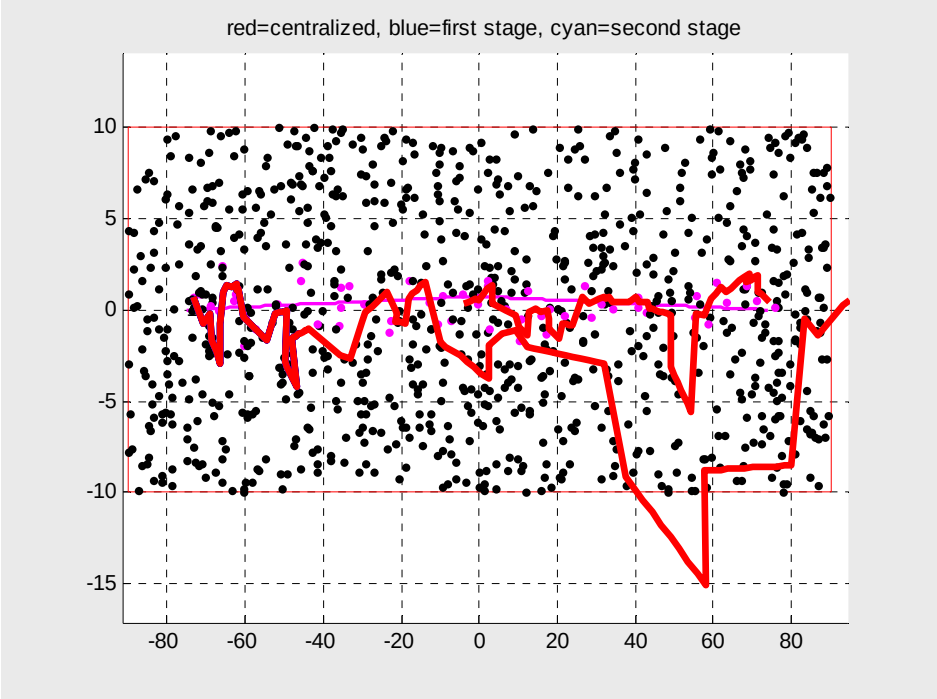


**Figure 3.3: The dim-target problem. Target trajectories (magenta), contact data (black), single-stage tracking (red).**

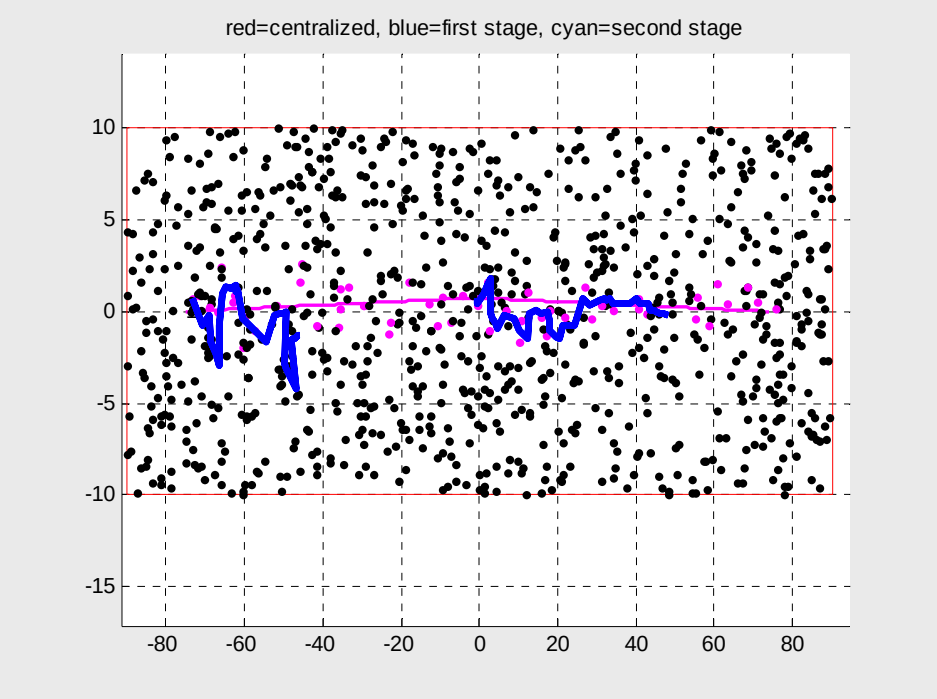


**Figure 3.4: The dim-target problem. Target trajectories (magenta), contact data (black), low-process-noise tracking (blue).**

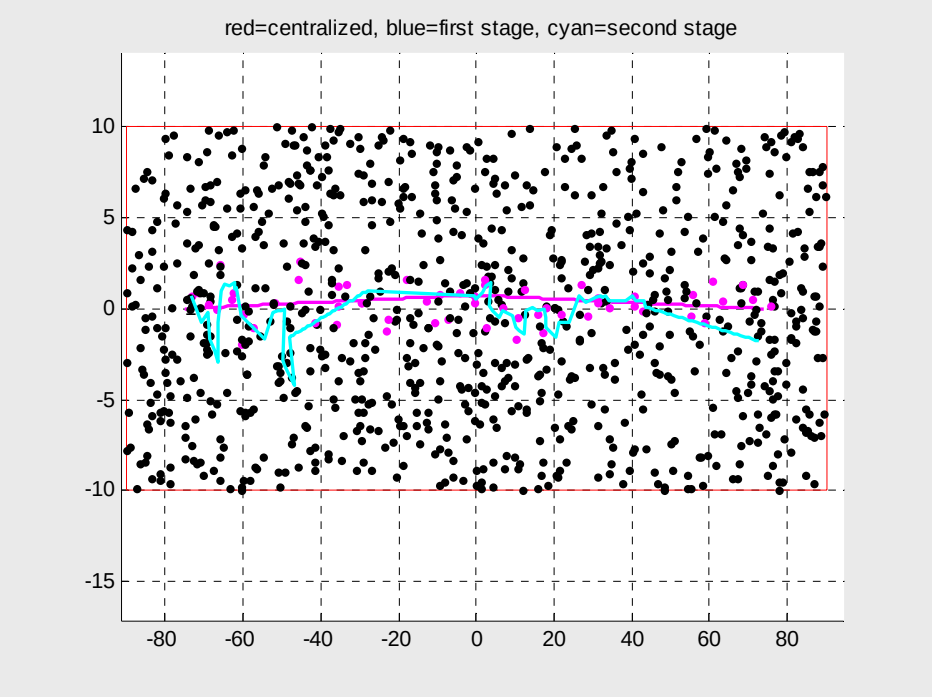


**Figure 3.5: The dim-target problem. Target trajectories (magenta), contact data (black), second-stage tracking (cyan) in *low-q track – high-q track* architecture.**

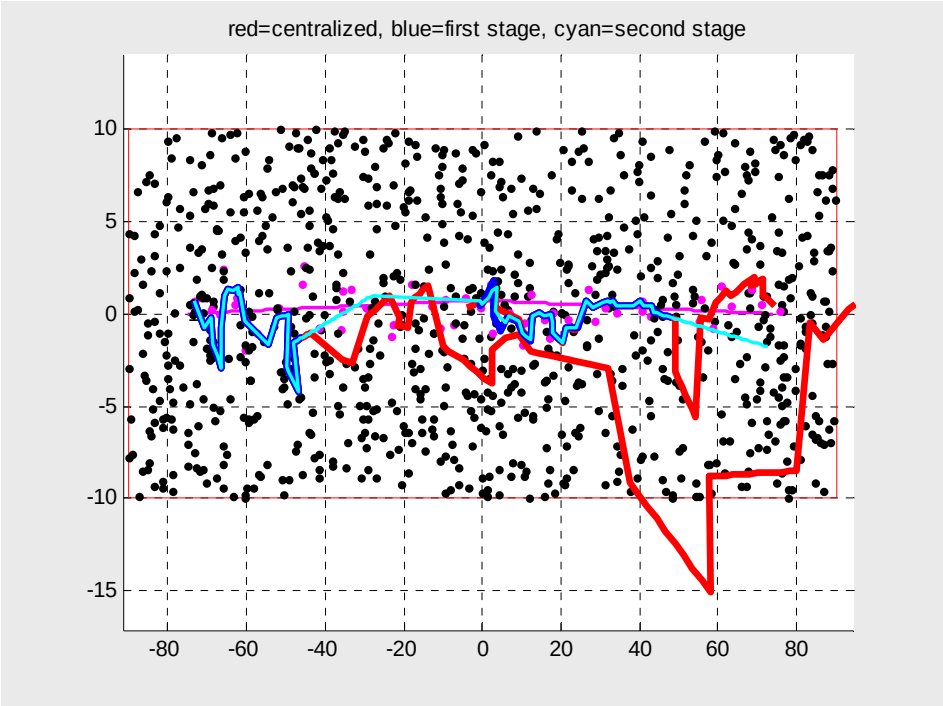


**Figure 3.6: The dim-target problem: aggregate results. Target trajectories (magenta), contact data (black), low-process-noise tracking (blue), second-stage tracking (cyan) in *low-q track – high-q track* architecture.**

## 3.4 Track merging

Automatic tracking often results in track fragmentation and redundant tracks on the same target. This may be caused by sensor limitations (missed detections, high false contact rate, unresolved measurement, redundant measurements) or tracker limitations. It is of interest to develop schemes to improve track continuity.

Our approach to this problem is to consider a post-tracker, track-merging algorithm. There are a number of reasons for choosing this two-stage processing paradigm as opposed to seeking to develop an enhanced, single-stage tracking solution:

- This is a simpler approach as it does not require changing the fundamental assumption that targets give rise to at most one measurement per scan;
- More aggressive fusion (in this context, allowing for multiple target returns from the same object) is less error prone in downstream processing in which false returns are largely absent;
- The tracker is scan-based, while our post-processing allows for batch analysis.

Simplifying assumptions:

- Single-sensor, single-footprint formulation; the general case will involve a multi-sensor, multi-footprint formulation;
- Upstream tracker involves hard data association and sensor measurement information is available at output (correspondingly, terminal track coasts are removed);
- No prior distribution on number of targets.

We develop a sub-optimal, greedy fusion approach as the optimal solution may be computationally intractable for a large number of tracks. We assume knowledge of the following:

- *Target kinematic model* and *sensor measurement model* that allow for the evaluation of $p\left(x_i \mid x^{i-1}\right)$, where $x^{i-1}$ is the measurement (and missed detection) sequence up to and including time $t_{i-1}$;
- A s*ensor detection model* for the number of returns per target per scan at time $t_i$. In a more general form, this model is the convolution of *Bernoulli* and *Poisson* distributions, allowing for a target-originated contact with probability $P_D$ as well as a Poisson-distributed number of false returns. The distribution may be simplified by limiting to one the number of extraneous returns (with probability $P_{FA}$); accordingly, we may then use the *multinomial* distribution as follows: $p_m(0) = (1-P_D)(1-P_{FA})$, $p_m(1) = P_D(1-P_{FA}) + P_{FA}(1-P_D)$, and $p_m(2) = P_D P_{FA}$.

Note that the sensor model applies *downstream* of target tracking, and as such accounts for tracker inaccuracies that give rise to redundant measurements. Thus, $P_{FA}$ reflects sensor measurement redundancies as well as false contacts that are associated to target tracks through tracker processing.

### 3.4.1 Track data without sensor measurements: the case of partial information and linear dynamics and measurements

Most tracking systems do not provide upstream sensor measurement information. In fact, for those trackers that utilize soft data association, generally there are multiple sensor measurements that give rise to each track update. Thus, it is of interest to extend the basic track-merging approach to account for these cases. As an intermediate case, trackers may provide *partial* sensor measurement information; namely, an indication as to where a given track state constitutes a *predicted* state (i.e. track coast) or *updated* state (i.e. measurement available).

We will focus on the case of partial measurement information and linear dynamical and measurement models. In this case, provided that tracker filter parameters are known and that there is exactly one measurement associated with each track update, pseudo-measurements can be derived that correspond exactly to the upstream measurements.

Let the known sequence of state estimates be given by $(X(1|1), X(2|2),...)$, and let $z = (z_1, z_2,...)$ be the measurement indicator sequence, i.e. $z_i = 1$ if there is a measurement at $t_i$, and $z_i = 0$ otherwise. Assume that the target dynamical model and sensor measurement model are known:

$$X_{k+1} = A_k X_k + w_k, w_k \sim N(0, Q_k), \tag{3.1}$$

$$Z_{k+1} = C_k X_k + v_k, w_k \sim N(0, R_k). \tag{3.2}$$

Assume $C_k = [C_{1,k} \quad C_{2,k}]$ with $C_{1,k} > 0$ and $C_{2,k} = 0$. Correspondingly, let $X(k|k) = [X_1(k|k) \quad X_2(k|k)]'$. Let $V$ be the covariance prior for the unmeasured portion of the state vector; as with the target and sensor models, we assume this filter parameter to be known. Manipulation of the Kalman filter equations leads directly to the measurement-reconstruction equations.

First, the filter covariance expressions can be reconstructed without filter state estimates as follows:

$$P(1|1) = \begin{bmatrix} C_{1,1}^{-1} R C_{1,1}^{-1^T} & 0 \\ 0 & V \end{bmatrix} Z_1 = C_{1,1}^{-1}. \tag{3.3}$$

$$P(k+1|k) = A_k P(k|k) A_k' + Q_k, \tag{3.4}$$

$$L_{k+1} = P(k+1|k) C_{k+1}' (C_{k+1} P(k+1|k) C_{k+1}' + R_k)^{-1}, \tag{3.5}$$

$$P(k+1|k+1) = (I - 1[z_{k+1} = 1] L_{k+1} C_{k+1}) P(k+1|k). \tag{3.6}$$

Next, measurement reconstruction is as follows; note that equation (8) applies when $z_{k+1} = 1$.

$$Z_1 = C_{1,1}^{-1} X_1(1|1), \tag{3.7}$$

$$Z_{k+1} = (P(k+1|k) + R_k) P^{-1}(k+1|k) \left( X(k+1|k+1) + \left( I - P(k+1|k) C_k' (P(k+1|k) + R_k)^{-1} \right) A_k X(k|k) \right). \tag{3.8}$$

### 3.4.2 Track scores

Let track *j* be given by a sequence of associated measurements $(x_1, x_2, ...)$ defined on $(t_1, t_2, ...)$. We define $x_i = \phi$ when no measurement exists at time $t_i$. Further, let $s(j) = \min_i \{t_i \mid x_i \neq \phi\}$ and $f(j) = \max_i \{t_i \mid x_i \neq \phi\}$. The track score $c(j)$ is given by the following, where $x^{i-1}$ denotes all measurements up to and including time $t_{i-1}$:

$$c(j) = -\log \prod_{i=s(j)}^{f(j)} \left\{ 1[x_i \neq \phi] p_m(1) p(x_i \mid x^{i-1}) + 1[x_i = \phi] p_m(0) \right\}. \tag{3.9}$$

In equation (3.1) we have $p(x_1) = g(0, R_1)$, where *g* is the Gaussian *probability density function* (pdf). Further, $p_m(\cdot)$ is the multinomial distribution as noted previously.

More generally, let track *j* be given by a sequence of associated measurements $(x_{1,1}, x_{1,2}, ..., x_{2,1}, ..., x_{i,k}, ...)$ where $n_i \geq 0$ measurements may exist at time $t_i$. In the case of no measurements at time $t_i$, we have $x_{i,1} = \phi$. The track score $c(j)$ is given by:

$$c(j) = -\log \prod_{i=s(j)}^{f(j)} \left\{ 1[x_{i,1} \neq \phi] p_m(n_i) \prod_{k=2}^{n_i} p(x_{i,k} \mid x^{i-1}, x_{i,1}, ... x_{i,k-1}) p(x_{i,1} \mid x^{i-1}) + 1[x_{i,1} = \phi] p_m(0) \right\}. \tag{3.10}$$

In equation (3.10), we have $p(x_{1,1}) = g(0, R_1)$. Simplifying the notation by suppressing the redundant-measurement index *i*, the kinematic-residual cost term is given by:

$$p(x_{k+1} \mid x^k) = f(x_{k+1} - C_{k+1} X(k+1 \mid k), C_{k+1} P(k+1 \mid k) C'_{k+1} + R_{k+1}). \tag{3.11}$$

Note that, in general, the track score depends on the ordering of multiple measurements at the same time. We neglect this and consider an arbitrary ordering of such measurement. (In the case of linear measurements, the ordering does not impact the track score.)

### 3.4.3 Greedy track merging

Let *N* be the number of tracks of interest, and let each track *j* have associated cost $c(j)$. We consider an *N-by-N* matrix *C* of fused-track costs, where the *ij*th element $c_{ij}$ is given by $c(l) - c(i) - c(j)$. In turn, track $l(i, j)$ is defined by the merged, time-ordered sequences of measurements in tracks *i* and *j*. The diagonal elements of *C* are set to zero: $c_{jj} = 0, j = 1, ...N$. Each matrix element $c_{ij}$ represents the cost of replacing tracks *i* and *j* with the corresponding track $l(i, j)$.

Having generated matrix *C*, we identify its smallest negative matrix element $c_{\hat{i}\hat{j}}$. Correspondingly, we replace tracks $\hat{i}$ and $\hat{j}$ by $l(\hat{i}, \hat{j})$. This leads to a set of *N*-1 tracks, for which a new matrix *C* is determined. The procedure is iterative, and terminates when no non-negative matrix elements remain.

Note that the track fusion methodology defined here avoids the enumeration of the $2^N - 1$ *local* track hypotheses to be considered. Thus, there is no guarantee that the resulting set of fused tracks corresponds to the optimal set of local track hypotheses. In principle, if $2^N - 1$ were not prohibitive, one could consider an LP-relaxation or Lagrangian relaxation approach to determine the optimal set of local hypotheses [9-10]. Track-oriented relaxation approaches obviate the need for considering global hypotheses; indeed, given *N* tracks, there are $B_N$ ways to partition these, where the Bell number $B_N$ grows very rapidly as a function of *N* [11].

### 3.4.4 Examples with two synthetically-generated tracks

Let us examine a simple example in which a linear target trajectory gives rise to two overlapping-in-time tracks. Following the methodology defined above, it is of interest to investigate under what conditions the tracks are merged. The exact scenario characteristics are summarized in table 3.2.

**Table 3.2: Scenario characteristics for the two-track example.**

| | |
|---|---|
| Sensor revisit time | 1sec |
| Sensor measurement covariance matrix | $\begin{bmatrix} 1 & 0 \\ 0 & 1 \end{bmatrix} \mathrm{m}^2$ |
| Sensor detection probability | $P_D = 0.9$ |
| Sensor revisit time | 1sec |
| Duration of tracks | 60 scans |
| Duration of track overlap | $s$ scans |
| Track displacement bias | $d$ m |
| Tracker kinematic process noise | $0.01\mathrm{m}^2\mathrm{s}^{-3}$ |
| Tracker velocity prior covariance | $\begin{bmatrix} 1 & 0 \\ 0 & 1 \end{bmatrix} \mathrm{m}^2\mathrm{s}^{-2}$ |
| Extraneous measurement probability | $P_{FA}$ |

A scenario realization is illustrated in figures 3.7-3.8, with $d$=1m, $s$=3, and $P_{FA} = 0.1$.

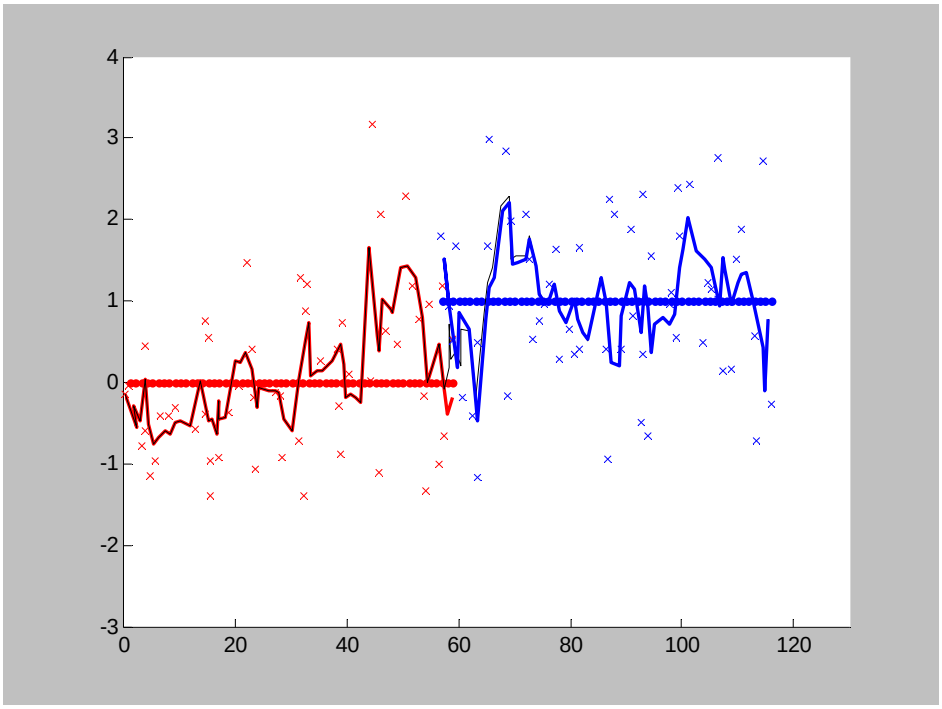


**Figure 3.7 Two-track example. Nominal target locations are red and blue dots, sensor measurements are crosses, track segments are trajectories, fused track is black trajectory.**

Figure 3.9 provides Monte Carlo results. Each data point is based on 20 realizations. As expected, we find that tracks that have a temporal gap generally will not fuse, and likewise tracks with significant temporal overlap will not fuse. The highest fusion likelihood is achieved when there is neither a temporal overlap nor a temporal gap. As the kinematic discrepancy (track displacement bias $d$) is reduced or the

redundancy parameter is increased (extraneous measurement probability $P_{FA}$), fusion is more likely to lead to improved track scores.

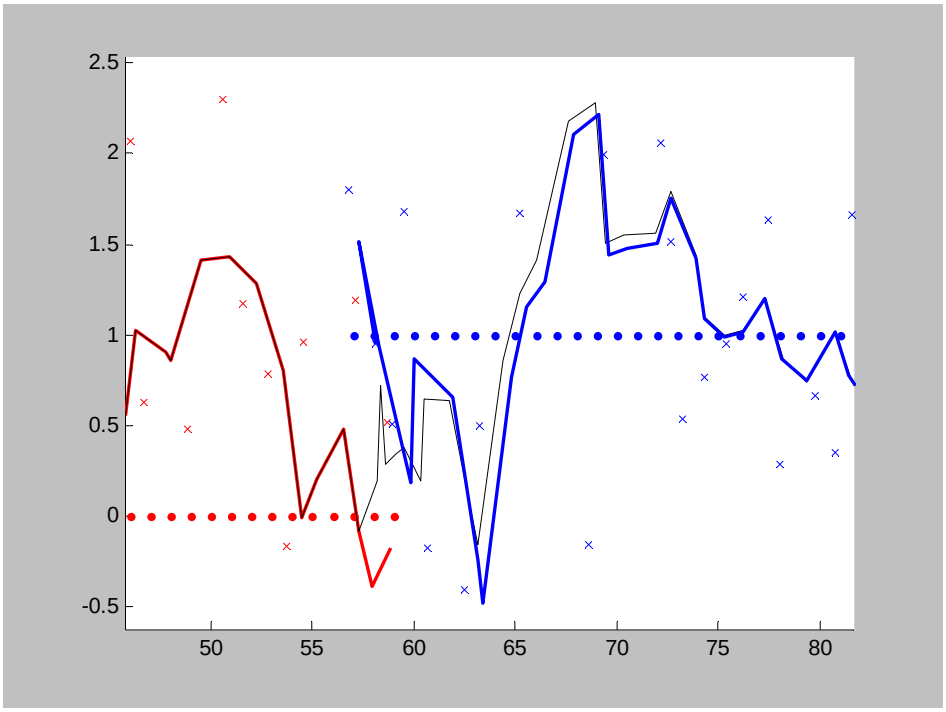


**Figure 3.8: Close-up of track overlap in figure 3.7.**

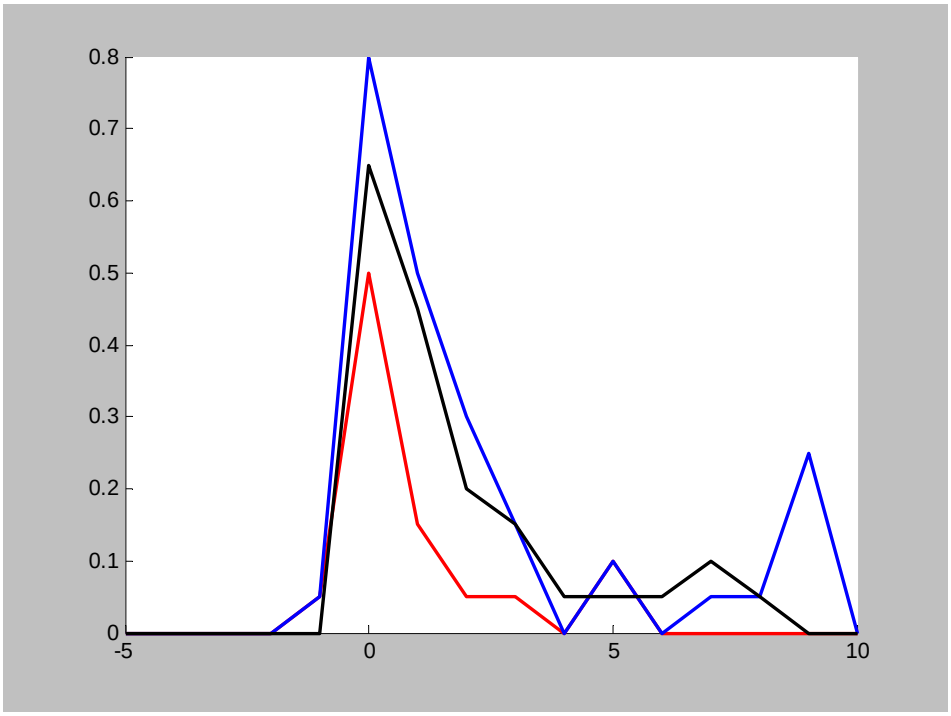


**Figure 3.9: Baseline results (*d*=2, $P_{FA} = 0.1$) in red; variations leading to higher probability of track-score improvement through fusion: first variation (*d*=1, $P_{FA} = 0.1$) in blue and second variation (*d*=2, $P_{FA} = 0.2$) in black.**

It is worth noting that in the special case of two point-tracks, these will not fuse regardless of whether they is overlap, a temporal gap, or neither. The best-scoring fusion situation is where there is neither overlap nor a gap. Nonetheless, even in this instance, the kinematic-filter score given by equation (3.10) is slightly lower than in the case of a second track initiation. The result is a reasonable one: tracks should fuse only when the detection and kinematic characteristics of the scenario are such as to justify modification of the upstream tracker output.

In general, out-of-phase measurements (i.e. coasts on one track when the other has updates) and single-track maneuvers in conjunction with track fragmentation will *increase* the likelihood that track merging will be performed. Such instances emerge in more complex, data-driven track realizations than those examined in this section. Thus, more comprehensive analysis of track merging performance is required with tracker executions based on simulated sensor data.

To conclude, our approach to track merging accounts for target kinematic characteristics, sensor detection and localization characteristics, and the impact of target tracking on redundant measurements. Further work includes: (1) analysis of the performance benefits of track merging with simulation-based tracker runs; (2) treatment of the general case of legacy track data and a quantification of the corresponding performance degradation; and (3) development of a scan-based track-merging methodology, for use in real-time tracking applications.

# 4 CONCLUSIONS

Estimation and detection theory provide a theoretical underpinning for a wide variety of problems that, taken as a whole, constitute the target tracking challenge. These notes provide a brief taxonomy of approaches to this challenge, and move on to discuss specific results on the *target cardinality problem* and in *multi-stage tracking*; the latter in particular is an area of active research in which the author has been engaged for many years. Multi-stage approaches to tracking are often simpler, more robust, and higher performing than highly sophisticated single-stage processing algorithms. We hope to encourage more research on fusion architectures, as we believe this topic constitutes a fruitful area for significant advances in surveillance capabilities for a wide variety of security and defense applications.

# 5 REFERENCES

[1] H. Tijms, *Stochastic Models: An Algorithmic Approach*, Wiley, 1994.

[2] B. McCue, A Justification of a Negative Binomial Model for Target Sightings, *Military Operations Research*, vol. 8(4), 2003.

[3] K. Bryan and C. Carthel, A Bayesian approach to predicting an unknown number of targets based on sensor performance, in *Proceedings of the 9th International Conference on Information Fusion*, Florence Italy, July 2006.

[4] A. Washburn, Katz Distributions, with Applications to Minefield Clearance, *Naval Postgraduate School Technical Report NPS-OR-96-003*, March 1996.

[5] S. Coraluppi and C. Carthel, Multi-Stage Data Fusion in Military Surveillance Systems, in *NATO RTO SET-133 Lecture Series on Multistatic Surveillance and Reconnaissance: Sensor, Signals and Data Fusion*, April 2009.

[6] C. Carthel and S. Coraluppi, An ML-MHT Approach to Tracking Dim Targets in Large Sensor Networks, to appear in *Proceedings of the 13th International Conference on Information Fusion*, Edinburgh, Scotland, July 2010.

[7] C. Carthel, S. Coraluppi, K. Bryan, and G. Arcieri, Wide-Area Feature-Aided Tracking with Intermittent Multi-Sensor Data, in *Proceedings of the SPIE Conference on Signal and Data Processing of Small Targets*, Orlando FL, USA, April 2010.

[8] C.-Y. Chong, G. Castanon, N. Cooprider, S. Mori, R. Ravichandran, and R. Macior, Efficient Multiple Hypothesis Tracking by Track Segment Graph, in *Proceedings of the 12th International Conference on Information Fusion*, Seattle WA, USA, July 2009.

[9] S. Coraluppi and C. Carthel, Recursive Track Fusion for Multi-Sensor Surveillance, *Information Fusion*, vol. 5(1), March 2004.

[10] A. Poore et al, Data Association Problems Posed as Multidimensional Assignment Problems: Problem Formulation and Numerical Simulations, *SPIE Conference on Signal and data Processing of Small Targets*, April 1993.

[11] http://en.wikipedia.org/wiki/Bell_numbers